Desalination and Water Treatment
www.deswater.com

17 (2010) 294–303
May

1944-3994/1944-3986
doi: 10.5004/dwt.2010.1732

Solid-liquid phase separation of poly-4-methyl-1-pentene/diluent system via thermally induced phase separation

Haijun Tao[a], Qin Xia[a], Shuangjun Chen[a], Jun Zhang[a]*, Xiaolin Wang[b]

[a]*College of Materials Science and Engineering, Nanjing University of Technology, Nanjing 210009, China*
Tel. +862583587264; Fax +862583240205; email: zhangjun@njut.edu.cn
[b]*Department of Chemical Engineering, Tsinghua University, Beijing 100084, China*

Received 24 July 2009; accepted 25 November 2009

ABSTRACT

Poly-4-methyl-1-pentene (PMP) microporous membranes were prepared via thermally induced phase separation (TIPS) with dioctyl adipate (DOA) as the diluent. Solid-liquid phase separation happened to this PMP/DOA system because of the weak interaction between them, which resulted in the spherulitic structure. Unique and obvious spherulites were formed at low PMP concentration system or low quenching temperature, while the spherulites were destroyed and impinged at high PMP concentration or high quenching temperature. Differential scanning calorimetry (DSC) and wide-angle X-ray diffraction (WAXD) were used to analyze the crystallization of PMP in the PMP/DOA system via TIPS. The increase of the PMP concentration delayed the crystallization of PMP, which was inferred from the results of both the isothermal and non-isothermal crystallization of the PMP/DOA system. The crystallization was faster and had more effect on the ultimate membrane morphology when the quenching temperature decreased. Double endotherm peaks emerged on DSC melting curves of PMP/DOA quenched samples were owing to the crystals of different extent formed in primary crystallization and further crystallization during TIPS.

Keywords: Thermally induced phase separation; Poly-4-methyl-1-pentene; Microporous membrane; Crystallization; Double endotherm peaks

1. Introduction

Poly(4-methyl-1-pentene) (PMP) is a semi-crystalline polyolefin with a number of interesting properties, such as low density, higher thermal stability, chemical resistance, optical transparency and high gas permeability [1]. It is of practical importance as a membrane-making polymer [2,3]. Thermally induced phase separation (TIPS) as a novel method has been used to prepare PMP microporous membrane. The phase separation and polymer crystallization behavior interacted with diluents were key factors for the preparation of PMP microporous membrane [4,5].

The typical solid-liquid (S-L) phase separation [6–9] will happen when the interaction between the polymer and the diluent is a little strong in which there is no liquid-liquid (L-L) phase separation region in the phase separation diagram. Matsuyama et al. [10] gave the phase diagram of the S-L phase separation system of HDPE/liquid paraffin, in which only the crystallization temperatures were observed but not the cloud points. The poly(ethylene-co-vinyl alcohol) (EVOH) [11,12] membrane also could be prepared by S-L phase separation via TIPS and the content of EVOH had effect on the membrane structure.

*Corresponding author

Presented at the Fifth Conference of the Aseanian Membrane Society Aseania 2009 "Recent Progress in Membrane Science and Technology", 12–14 July 2009, Kobe, Japan.

When PVDF microporous membranes were prepared via TIPS S-L phase separation occurred in the system of PVDF/dibutyl-phthalate (DBP), mainly resulting in spherulitic structure in Li and Lu's report [13] or fuzzy sphere structure reported by Lloyd et al. [6]. Besides, S-L phase separation results in the structure of spherulites in two cases: First, if the polymer concentration was higher than the monotectic point on the phase separation diagram S-L phase separation was a common result. Spherulitic structures with or without some micropores were observed resulted from S-L phase separation when the polymer concentration was more than 30 wt% in ethylene-acrylic acid co-polymer (EAA)/dioctyl phthalate (DOP) system [14], or more than 30 wt% in low density polyethylene (LDPE)/diphenyl ester (DPE) system [15] and more than 30 wt% in EAA/DPE system [16]. The other is quenching of the low polymer concentration systems below the crystallization temperatures with a rapid cooling rate in the L-L region. However, if the cooling rate was not so rapid there would be the crystallization of polymer and the occurrence of L-L phase separation simultaneously.

S-L phase separation may occur during non-isothermal or isothermal crystallization process of polymer/diluents. Lloyd et al. [6] found that spherulites or structure of polymer particles linked by tie fibrils were formed in the system of polypropylene (PP)/mineral oil. Larger spherulites were formed with slower cooling rate, and the quenching resulted in smaller spherulites than controlled cooling rate. However, the polymer concentration had no significant effect on the spherulitic size in S-L phase separation. Kim et al. [9] concluded that the diluent mobility and crystallization could affect the S-L TIPS membrane structure. Nucleating agent would affect the PP crystallization and then the membrane structure by S-L phase separation [8]. In addition, leafy structure was observed in 19 wt% high-density polyethylene (HDPE)/mineral oil system when quenched from 175°C to 30°C [6].

In our previous studies [4,5], L-L phase separation occurred when dioctyl sebacate (DOS)/dimethyl phthalate (DMP) and DBP/DOP were used as diluents, and well-defined cellular structure was formed because of the appropriate interaction between PMP and the diluents. However, in this paper another diluent dioctyl adipate (DOA) with a solubility parameter 17.6 $(J/cm^3)^{1/2}$ close to the 16.8 $(J/cm^3)^{1/2}$ of PMP was used [17], resulting in a little stronger interaction. Typical S-L phase separation and the spherulitic structure were supposed to be formed during TIPS process. The crystallization behavior of PMP and the ultimate membrane morphology were also investigated.

2. Experimental

2.1. Materials

Membranes were prepared with the system of PMP/DOA. The polymer, PMP (MX-002) was purchased from Mitsui &Co., Ltd, Japan. DOA (CP) was supplied by Shandong Haihua Tianhe Organic Chemical Co., Ltd, China. Methanol (AR) and *i*-butanol (AR) were obtained from Shanghai Lingfeng Chemical Reagents Co., Ltd, China, and used without further purification.

2.2. Membrane preparation

Appropriate amounts of PMP and DOA were mixed in a test tube, which was placed into an oil bath kept at 250 ± 2°C with low stirring for 4 h. Then the mixture was cooled at ambient temperature for 30 min, yielding a solid PMP/DOA sample. The solid sample was chopped into small pieces, which were placed in a tailor-made test tube, a ram-type copper tube with the inner, outer diameters of 10 and 12 mm, respectively, sealed by the copper plunger. After reheating in an oven for 15 min at 250°C, the test tube was taken out to quench at the experimental temperature for a certain time, followed by quenching to 0°C immediately for solidification. Finally, the diluent was extracted from the membrane by methanol. The extractant was evaporated in a vacuum oven (ZK-82A, Shanghai Laboratory Apparatus Company, China) and the membrane was obtained.

2.3. Phase diagram

The pieces chopped from the samples above were used for phase diagram determination. The cloud points of PMP/DOA were supposed to be determined visually by noting the appearance of turbidity with the microscope. The relevant crystallization temperatures for the phase diagram were determined by Perkin-Elmer DSC-7C. The samples weighing 10 mg were sealed in an aluminum DSC pan, melted at 250°C, and then cooled to 50°C at the rate of 5°C/min. The onset of the exothermic peak during the cooling was taken as the dynamic crystallization temperature.

2.4. Characterization of the membrane

2.4.1. Scanning electron microscopy (SEM)

SEM micrographs were taken by an S-3000N (Hitachi, Japan) SEM. Each of the samples was fractured under liquid nitrogen, and coated with gold

using a sputtering coater, and then the cross-section was scanned.

2.4.2. Porosity

The ultimate PMP membranes were immersed in *i*-butanol for 24 h, and weighed immediately after removing the *i*-butanol from the surface. The porosity (A_k) was calculated according to the following equation [14,18]:

$$A_k = \frac{\rho_1(W_2 - W_1)}{\rho_1 W_2 + (\rho_2 - \rho_1)W_1} \times 100\%, \quad (1)$$

where W_1 is the initial membrane weight; W_2 is the immersed membrane weight; ρ_1 is the density of PMP, taken as 0.83 g/cm^3 [19]; and ρ_2 is the density of *i*-butanol, taken as 0.80 g/cm^3.

2.5. Characterization of the polymer crystallization

2.5.1. Differential scanning calorimetry (DSC) analysis

PMP crystallization in the PMP/DOA system was followed through DSC measurement on a Perkin-Elmer DSC-7C (U.S.A.), and the endotherm peaks were recorded in order to fully characterize the thermal behavior. Measurements were made on about 10 mg solid polymer/diluents sample, heated from 50°C to 250°C at 10°C/min. The degree of crystallinity (X_c) was calculated according to the following equation [14,18]:

$$X_c = \Delta H_m/(\Delta H^*_m \times C), \quad (2)$$

where ΔH_m is the endothemic heat during the melting process and ΔH^*_m is the heat of fusion of a perfect crystal, taken as 117.2 J/g [19] for PMP. The C is the concentration of PMP in the polymer/diluents systems. For non-isothermally crystallization the sample was first melted at 250°C for 5 min and then the sample was cooled to 50°C at 5°C/min.

2.5.2. Wide-angle X-ray diffraction (WAXD) analysis

For WAXD measurement, additional samples of about 1 × 1 cm with the average thickness of about 0.1 mm were made at the same condition in which the membranes were made. Small pieces of the solid PMP/DOA sample were melted onto a microscope slides at 250°C, and quenched at a certain temperature, then quenched immediately to 0°C. The XRD-6000 (Shimadzu, Japan) was used in this study, with the 2θ ranging from 5° to 60° using CuK_α radial. For further analysis, the interplanar spacing d and the thickness of the lamellar crystal D values which represent the crystal grain size were calculated according to the Bragg and Scherrer equations respectively as Eq. (3) and Eq. (4) [20,21]:

$$d = \lambda/2\sin\theta, \quad (3)$$

$$D = k\lambda/\beta\cos\theta, \quad (4)$$

where λ is the wavelength of the X-ray, taken as 0.1542 nm, θ is the half scanning angle, k is Scherrer constant, taken as 0.89, and β is the full width at half maximum (FWHM) of the diffraction peak (measured in radian).

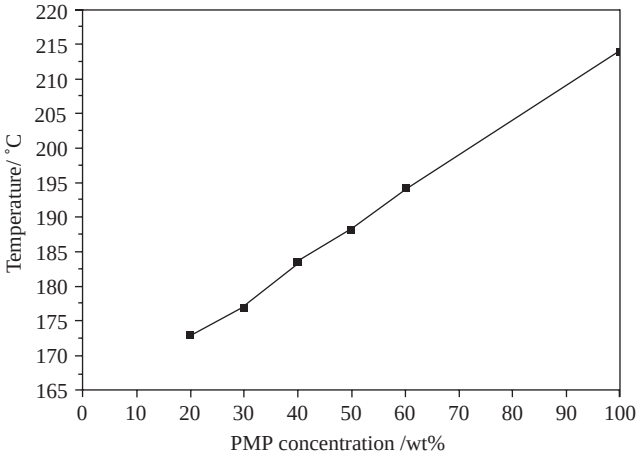

Fig. 1. Phase diagram of PMP/DOA system.

3. Results and discussion

3.1. Phase separation diagram

PMP/DOA solid mixtures were prepared in different PMP concentrations, including 20, 30, 40, 50 and 60 wt%. And the cloud points were meant to be measured to determine the phase diagram, but no cloud point was observed before the crystallization of PMP. About 10 mg PMP/DOA solid mixtures were sealed in the DSC pan to melt at 250°C for 5 min and then cooled at 5°C/min to crystallize. The plot of onset crystallization temperatures versus PMP concentration was shown in Fig. 1.

It could be found that the T_c increased nearly linearly with the increase of PMP concentration in the range of 20–100 wt%, which was a typical character of S-L phase separation [6–9]. So it was considered that S-L phase separation would occur in the PMP/DOA system when cooled.

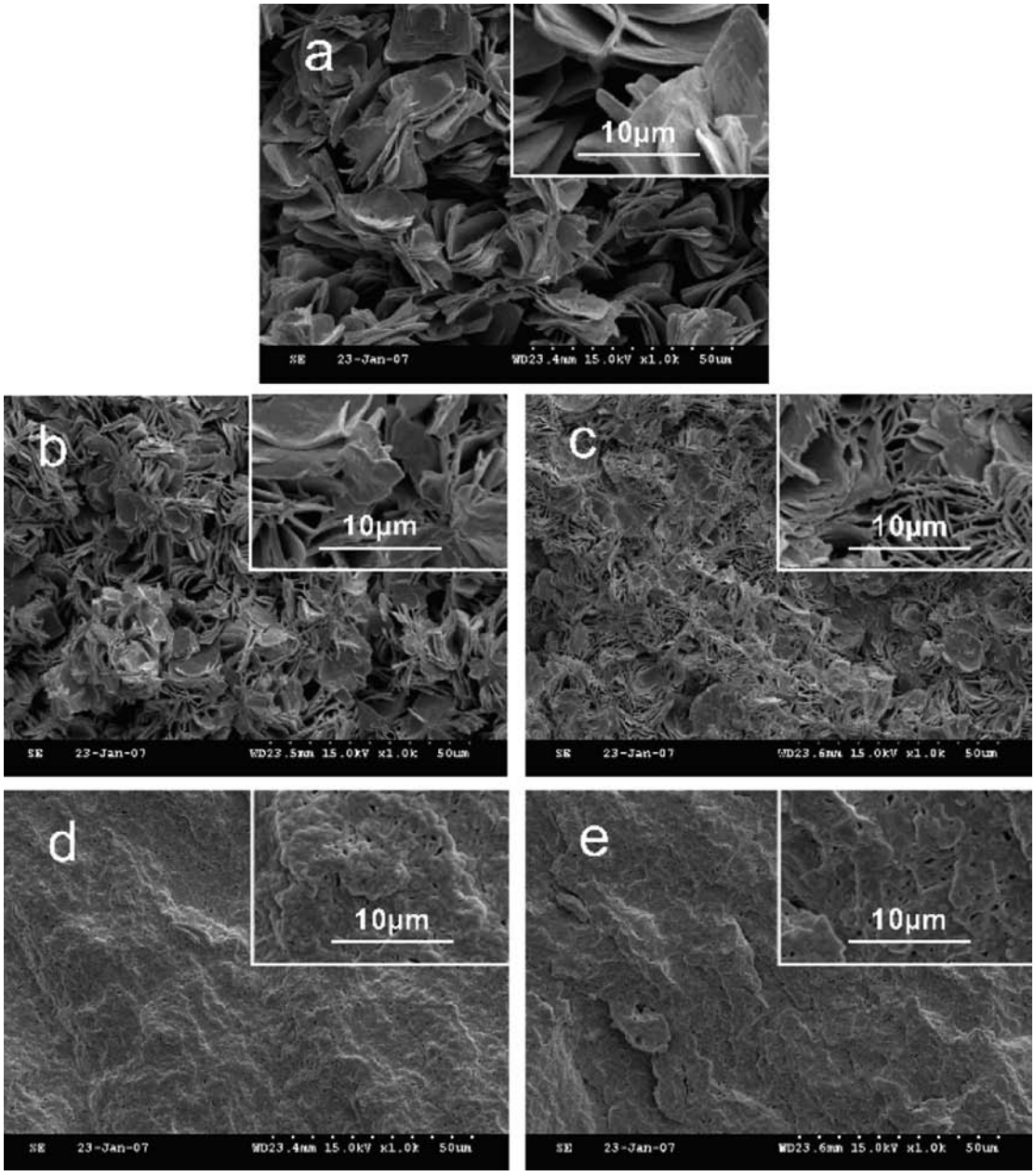

Fig. 2. Cross-section SEM micrographs of the PMP/DOA membranes with different concentrations quenched at 120°C for 15 min: a, 20 wt%; b, 30 wt%; c, 40 wt%; d, 50 wt%; e, 60 wt%.

3.2. Effect of PMP concentration on membrane morphology

The PMP/DOA systems of the PMP concentrations of 20, 30, 40, 50 and 60 wt% were melted and quenched at 120°C for 15 min to prepare PMP membranes. The cross-section SEM micrographs of the membranes were shown in Fig. 2. As shown in Fig. 2, there were no well-formed pores, but PMP crystallized when PMP concentration was changed. S-L phase separation occurred in the systems with PMP concentrations of 20, 30 and 40 wt% characterized by the lamellar crystals comprising the spherulites. As the concentration of PMP increased, the large voids between spherulites diminished and the spherulites became less discernible, and they impinged into a whole without any large void left at 50 and 60 wt%.

The size of the spherulites that composed by lamellar crystals decreased as the increase of PMP content. S-L phase separation happened when PMP/DOP quenched at 120°C by the crystallization of PMP molecular chains accompanied the ejection of diluent into

the inter-spherulites. On the one hand, there were more DOA molecules that could be ejected and then large voids formed in the inter-spherulite region at low PMP concentration. On the other hand, there was less diluent at high PMP concentration, and the mobility of DOA molecule would be much decreased because the viscosity increased much due to the high PMP concentration. The measured data of porosity also indicated the extent of the crystals' pinch. The porosities were 73.5%, 61.4%, 55.8%, 8.4% and 2.4%, respectively.

3.3. Effect of PMP concentration on PMP crystallization

3.3.1. Isothermal crystallization

The crystallization of polymer during S-L phase separation is much more important even dominant than that in L-L phase separation. The polymer would isothermally crystallize in the polymer/diluent system when quenching at a constant temperature, so the crystallization process and the ultimate crystals formed would have effect on the membrane morphology. The PMP/DOA samples with the PMP concentrations of 20, 30, 40, 50 and 60 wt%, as well as the pure PMP were melted at 250°C and then quenched at 120°C for 15 min for the DSC measurement. The DSC melting curves with the heating rate of 10°C/min were shown in Fig. 3 and the data were listed in detail in Table 1.

In Table 1 (also in Table 2), T_{p1} and T_{p2} are the abbreviated forms of the lower and higher melting peaks of PMP in the DSC melting traces. It could be found that the crystallinity of PMP in PMP/DOA system had no distinct increasing compared with the pure PMP, which was different from that in the PMP/DOS/DMP [13] system. The crystallinity of PMP in PMP/DOS/DMP system was enlarged because of the increased mobility of PMP molecular chains with the presence of DOS and DMP. However, the diluent DOA had larger interaction with PMP molecular chains because their solubility parameters were close, 16.8 $(J/cm^3)^{1/2}$ of PMP and 17.6 $(J/cm^3)^{1/2}$ of DOA, while that of DOS/DMP was 19.5 $(J/cm^3)^{1/2}$. What's more, the viscosity of the polymer/solvent system was increased in a good solvent [21]. Therefore, the mobility of PMP molecular chains was difficult and the arrangement of PMP chains into crystal lattice was hard too. With the increasing of PMP concentration from 20 to 30, 40, 50 and 60 wt% in PMP/DOA system, the crystallinity of PMP decreased, although a little. At the same time there were double endotherm peaks on the DSC melting curves of the 20, 30 and 40 wt% systems, with both the first low temperature peak and the second high temperature moving to higher temperature. As the concentration increased to 50 and 60 wt% in PMP/DOA system as well as the pure PMP only one melting peak emerged. The only melting peak also moved to higher temperature in these cases of high PMP concentration. The double endotherm peaks happened to the systems of low PMP concentration were similar to that happened in PMP/DOS/DMP.

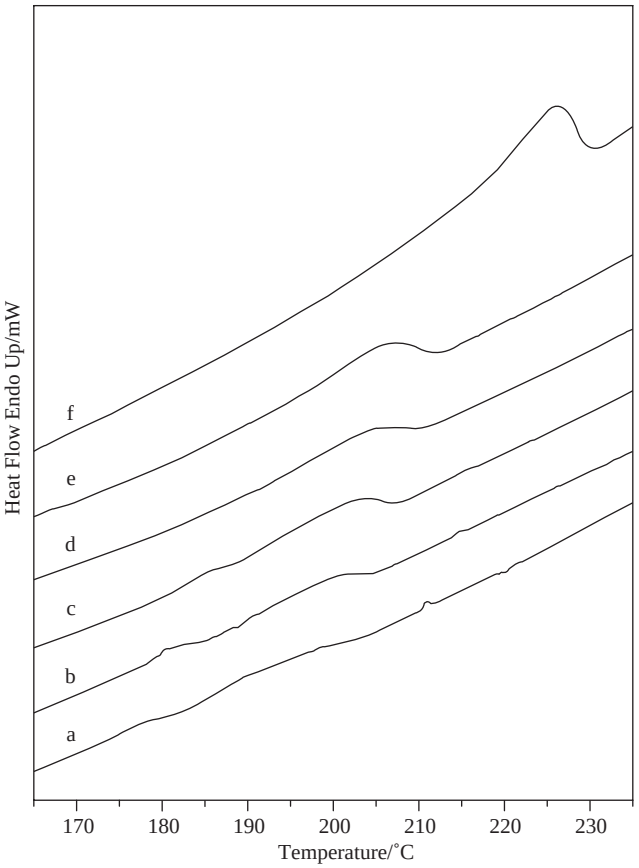

Fig. 3. DSC melting traces of PMP/DOA samples of different concentrations quenched at 120°C for 15 min (heating rate 10°C /min): a, 20 wt%; b, 30 wt%; c, 40 wt%; d, 50 wt%; e, 60 wt%; f, pure PMP.

Table 1
The detailed data of DSC melting traces in Fig. 3

Samples	T_m/°C		ΔH_m/J g^{-1}	X_c/%
	T_{p1}	T_{p2}		
20 wt%	177.4	195.5	2.7	11.5
30 wt %	181.2	200.5	3.3	9.4
40 wt %	184.9	203.1	4.6	9.8
50 wt %	–*	204.9	4.2	7.2
60 wt %	–	206.9	6.0	8.5
100 wt%	–	226.4	11.9	10.2

*only one melting peak.

Table 2
The detailed data of DSC melting traces in Fig. 5

Samples	T_m/°C		ΔH_m/J g^{-1}
	T_{p1}	T_{p2}	
5°C/min	178.8	196.1	1.9
10°C/min	179.9	197.4	3.3
15°C/min	181.2	199.2	3.6
20°C/min	182.5	200.9	4.1

The quenching step of TIPS was also an isotherm crystallization of the polymer. The double endotherm peaks of the cases with the concentrations of 20, 30 and 40 wt% quenched at 120°C were further concerned in this section. All the five quenched PMP/DOA samples at 120°C were scanned by XRD-6000 and the WAXD patterns were shown in Fig. 4.

It was found that intensity peaks at 2θ of about 9.6°, 13.6°, 16.8° and 18.5° emerged for all the five samples. They were according to the crystallographic planes (200), (220), (212) and (321) of the crystal phase I of PMP, so there was no different crystal phases formed with different PMP concentrations although five crystal phases I, II, III, IV and V have been reported [22,23]. The 30 wt% PMP/DOA samples quenched at 120°C for 15 min were measured by DSC with different heating rates, 5, 10, 15 and 20°C/min. The results were shown in Fig. 5 and Table 2. There were double melting peaks on every DSC melting curve with the high melting peaks almost at the same position 200°C. However, the first melting peak moved to high temperature as the heating rate increased, resulting in the approaching of the two peaks. Meanwhile there was no increasing of the area of the melting peak at the cost of the other one, but both the area of the two melting peaks enlarged with the increasing of the heating rate. These were completely different from that of the melting-recrystallization-melting which was characterized by the enlarging of one melting peak at the cost of the other one as the heating rate increased [24]. The simultaneous increases of the two melting peaks were just because of the hysteresis during the DSC.

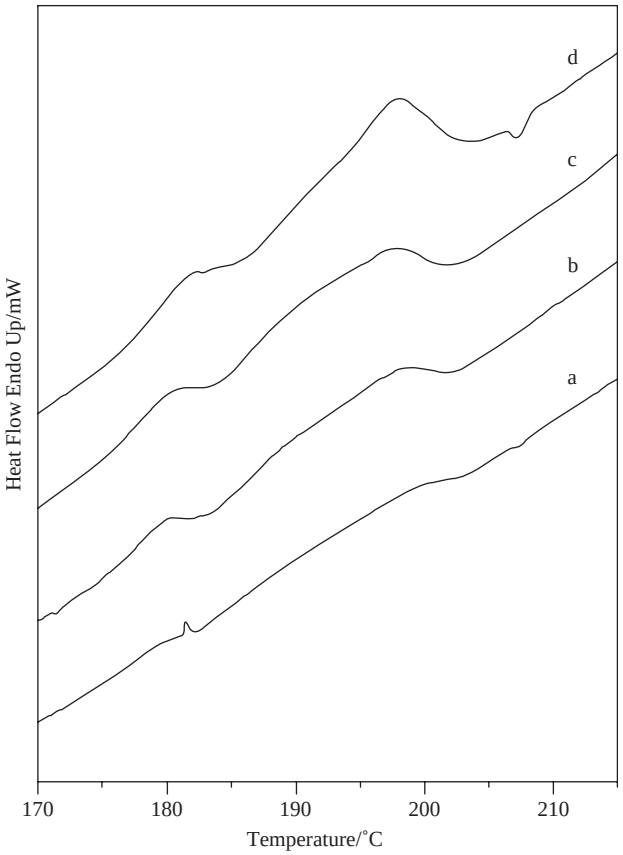

Fig. 5. DSC melting traces with different heating rates of 30 wt% PMP/DOA quenched at 120°C for 15 min: a, 5°C/min; b, 10°C/min; c, 15°C/min; d, 20°C/min.

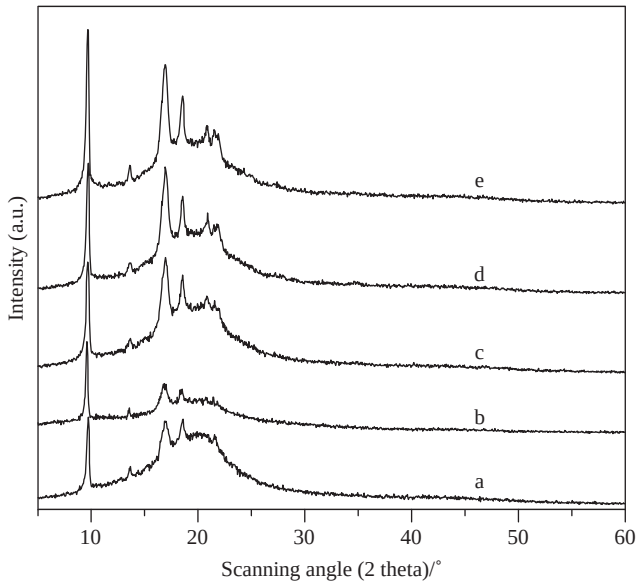

Fig. 4. WAXD patterns of PMP/DOA samples of different concentrations quenched at 120°C for 15 min: a, 20 wt%; b, 30 wt%; c, 40 wt%; d, 50 wt%; e, 60 wt%.

In our previous study [5], primary crystallization and further crystallization of PMP happened when PMP was quenched because the isobutyls in PMP molecular chains blocked the mobility of PMP, which was similar to those concluded by Pakula [25], Zryd [26] and Medellin-Rodriguez [27,28]. When the sample was cooled, primary crystallization first happened easily and formed lamellar crystals of larger size or extent, leaving some branched and even some

segments randomly in the interlamellar regions. As the temperature decreased the further crystallization would occur in the inter-region of the lamellar crystals and crystals of smaller size or extent would be formed. These crystals of different sizes or extent would lead to different thermal stabilities and then different melting peaks on DSC curves emerged: the further crystals melted at low temperature while the primary crystals melted at high temperature. As discussed in Section 3.3.1, the interaction between PMP and DOA was stronger than that of PMP and DOS/DMP, so the crystallization especially the further crystallization would be more difficult. Thus, the disappearance of the low melting temperature of the 50 and 60 wt% PMP/DOA systems which was attributed to the much decrease or even disappearance of the further crystallization because of both the higher viscosity and the stronger interaction between PMP and DOA.

3.3.2. Non-isothermal crystallization

In this section non-isothermal crystallization of PMP in PMP/DOA system was performed in DSC by cooling the sample at 5°C/min after melting at 250°C for 5 min. The crystallization curves of the systems with PMP of 20, 30, 40, 50, 60 wt% and the pure PMP are shown in Fig. 6 and the data are listed in Table 3.

In Table 3, T_{onset}, T_{peak} and T_f are the abbreviated forms of the onset, peak and finish crystallization temperatures of PMP in the DSC cooling traces. And ΔT_c is the width of crystallization temperature range from onset to finish crystallization temperatures. ΔH_c is the directly calculated enthalpy. ΔH is of dividing ΔH_c by the PMP concentration (C) in mixture. The crystallization process was composed of initial nucleation and the following growth of crystals. The crystal growth rate depended much on the mobility of the polymer molecular chains. When cooled at 5°C/min by DSC, the cooling rate was much lower than that of quenching for polymer, so there would be longer time for PMP molecular chains to arrange into the crystal lattice. The onset crystallization temperature T_{onset} and the peak crystallization temperature T_{peak} were increased with the PMP concentration, as shown in Table 3. It was indicated that the crystallization started earlier in the high concentration system, like that the polymer molecular chains crystallized at a low cooling rate which induced the faster initial nucleation process. However, the crystallization uniformity characterized by the ΔT_c, was enlarged when PMP concentration increased, which meant that the higher concentration of PMP would get more inhomogeneous crystalline. Therefore the enlarged ΔT_c of the cases of 50 wt%, 60 wt% and the pure PMP should be owing to the much difficulty of the molecular mobility in high PMP concentration systems. It was reported that the PMP crystallized on heating [29]. The exothermal enthalpy, ΔH, was an indication of the extent of the crystallization. In Table 3, ΔH had a tendency to decease. This also meant that the whole crystallization process in the cases of 50 wt%,

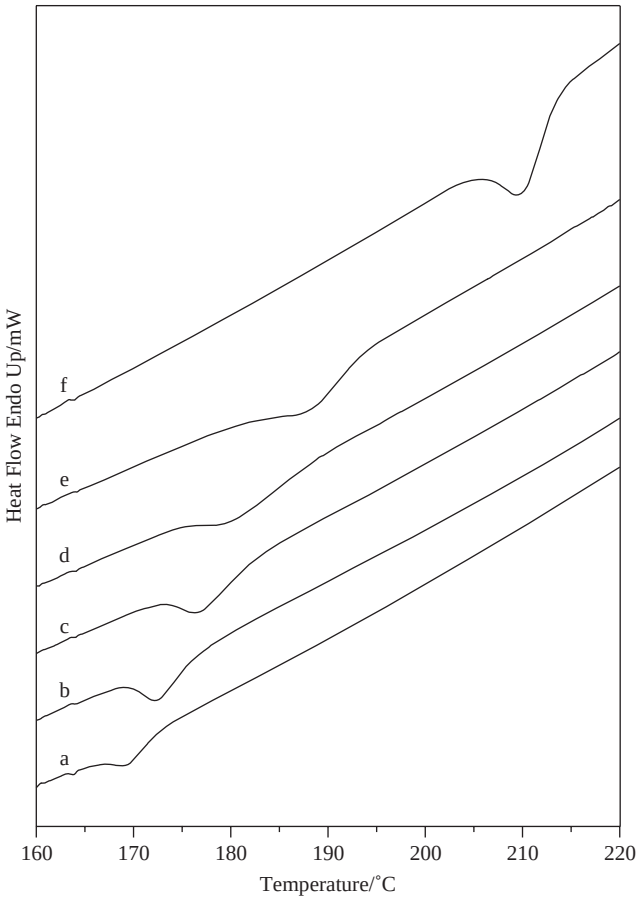

Fig. 6. DSC cooling traces of PMP/DOA samples of different concentrations (cooling rate 5°C/min): a, 20 wt%; b, 30 wt%; c, 40 wt%; d, 50 wt%; e, 60 wt%; f, pure PMP.

Table 3
The detailed data of DSC cooling traces in Fig. 6

Samples	T_c/°C			ΔH_c/J g^{-1}	ΔH/J g^{-1}
	T_{onset}	T_{peak}	$\triangle T_c$		
20 wt%	173.0	169.3	7.5	7.0	35.0
30 wt%	176.9	172.5	7.9	11.1	37.0
40 wt%	183.5	176.6	10.9	13.6	34.0
50 wt%	188.0	180.2	13.3	12.2	24.4
60 wt%	194.1	188.4	13.6	19.0	31.7
100 wt%	213.8	210.0	20.0	10.3	10.3

$\triangle T_c = T_{onset} - T_f$; $\Delta H = \Delta H_c/C$.

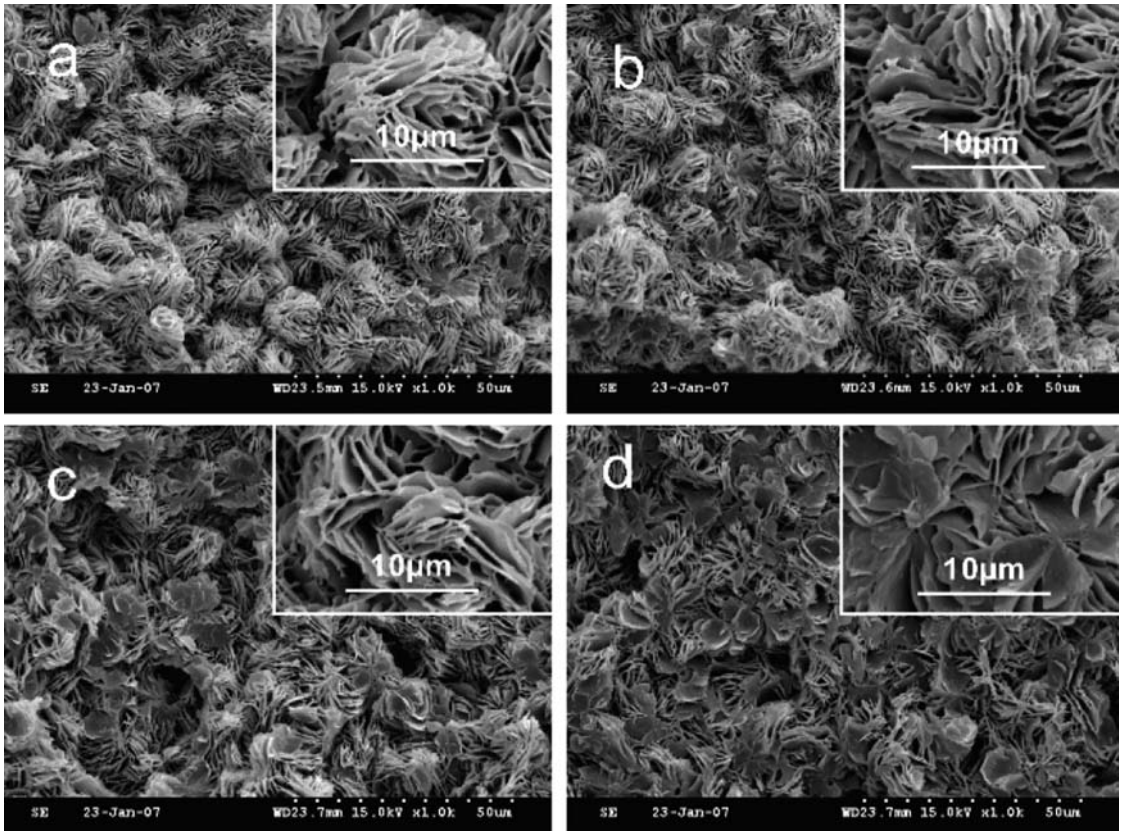

Fig. 7. SEM micrographs of 30 wt% PMP/DOA quenched at different temperatures: a, 60°C; b, 90°C; c, 120°C; d, 150°C.

60 wt% and pure PMP was difficult, which was in accordance with the change of ΔT_c.

3.4. Effect of quenching temperature on PMP membrane morphology

The 30 wt% PMP/DOA system was quenched at different temperatures including 60°C, 90°C, 120°C and 150°C. These four quenching temperatures were lower than the crystallization temperature in the phase diagram in Fig. 1. The SEM micrographs of the membrane fractured structures were shown in Fig. 7, 1,000 magnified on the left and 3,000 on the right. All the membranes were characterized by the crystal structure according to the SEM micrographs, spherulitic or leafy crystals.

Spherulites were more discernible with lower quenching temperature especially at 60°C. However, when the quenching temperature increased to 90°C the spherulites became less discernible and more impinged; when the quenching temperature was as high as 120°C and 150°C there were not complete spherulites but only leafy crystals. It was known that [8] the crystallization of the polymer was competed with phase separation when S-L phase separation occurred. At lower quenching temperature the polymer crystallized quickly while the mobility of diluent was limited. So the polymer molecule crystallized almost in a homogenous solution, resulting in well structured spherulites. As the quenching temperature raised, the crystallization was not so quick and the diluent could be ejected with better mobility when the crystallization happened, and then the solution intra and inter the spherulites would be different. The growth of spherulites was disturbed and imperfect spherulites formed. If the quenching temperature was high enough the phase separation would have much effect on the crystallization of polymer, in which the leafy crystals formed.

3.5. Effect of quenching temperature on PMP crystallization

The crystallization of PMP when the 30 wt% PMP/DOA system was quenched at 60°C, 90°C, 120°C and 150°C was studied by WAXD. The results of WAXD patterns shown in Fig. 8 indicated that only the phase I of PMP formed at different temperatures. The data derived from the WAXD patterns of the 30 wt%

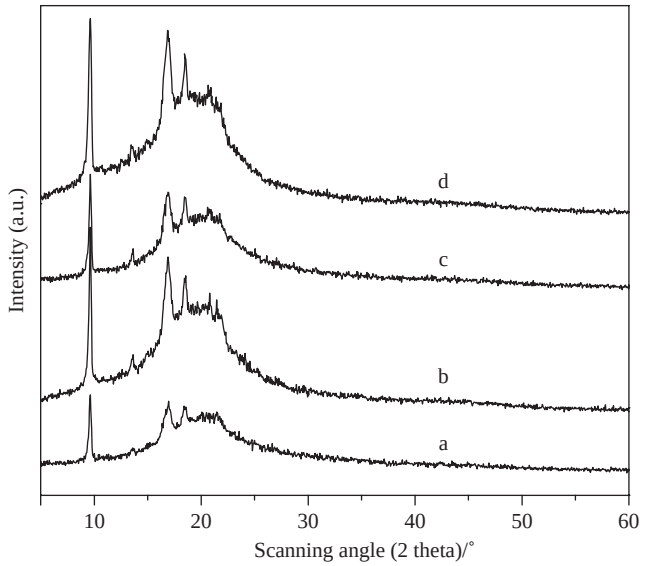

Fig. 8. WAXD patterns of 30 wt% PMP/DOA quenched at different temperatures for 15 min: a, 60°C; b, 90°C; c, 120°C; d, 150°C.

PMP/DOA samples quenched at different temperatures were listed in Table 4.

There was no obvious regulation of the intensity and the *d* values of PMP crystals although the PMP/DOA samples quenched at different temperatures by further analyses of these data. Medellin-Rodriguez [28] confirmed that the secondary crystalline structure would not give rise to the diffraction, just giving place to perceptive X-ray scattering but rather negligible X-ray diffraction. It might be concluded that the quenching temperature had no effect on the primary crystallization but the secondary crystallization. This consisted with the results of the DSC analyses. So the difference of the secondary crystallization resulting from the different quenching temperatures affected the DSC melting curves and the overall crystallinity, but not the diffractograms.

Table 4
The detailed data of the WAXD in Fig. 8

	Temperate (°C)			
Peaks	60	90	120	150
1 2θ (deg)	9.61	9.65	9.62	9.60
I/I_{max}*	100	100	100	100
D (Å)	9.20	9.16	9.18	9.21
D (nm)	28.48	44.89	29.57	22.95
2 2θ(deg)	13.56	13.55	13.56	13.52
I/I_{max}*	8	11	13	8
D (Å)	6.53	6.53	6.52	6.55
D (nm)	20.74	27.52	35.49	31.46
3 2θ(deg)	16.90	16.90	16.80	16.83
I/I_{max}*	52	53	53	63
D (Å)	5.24	5.24	5.27	5.26
D (nm)	12.86	-**	10.04	9.87
4 2θ (deg)	18.43	18.47	18.48	18.45
I/I_{max}*	35	34	38	43
D (Å)	4.80	4.80	4.80	4.81
D (nm)	14.97	17.39	19.44	13.98

*Comparative intensity to the strongest peak and **Can be calculated.

4. Conclusions

S-L phase separation happened to PMP/DOA system via TIPS, resulting in mainly the spherulitic structure not the well-formed pores. As the PMP concentration increased spherulites with discernable boundary were formed at low concentration while the spherulites impinged without any boundary at high concentration. For the 30 wt% PMP/DOA system unique and complete spherulites were formed at low quenching temperature, while destroyed, imperfect spherulites at high quenching temperature, because of different competitions between the phase separation and polymer crystallization. The increase of the PMP content was bad to the crystallization because of the raised viscosity according to the results of DSC of the quenched samples; in non-isothermal crystallization the effect of PMP concentration on the crystallization process was more remarkable, enlarging the whole crystallization time. The double endotherm peaks emerged on the DSC melting curves for the 30 wt% quenched samples were resulted from the primary and further crystallization occurred when quenched via TIPS. The PMP concentration and the quenching temperature had more effect on the further crystallization not the primary crystallization, indicated by the results of DSC and WAXD.

Acknowledgement

This work was supported by the National Basic Research Program of China under contract No. 2009CB623404.

References

[1] A.C. Puleo, D.R. Paul, P.K. Wong, Gas sorption and transport in semicrystalline poly(4-methyl-1-pentene), Polymer, 30 (1989) 1357–1366.
[2] K.H. Lee, S. Givens, D.B. Chase, J.F. Rabolt, Electrostatic polymer processing of isotactic Polymer, 47 (2006) 8013–8018.
[3] J.J.E. Samuel and S. Mohan, FTIR and FT Raman spectra and analysis of poly(4-methyl-1-pentene), Spectrochim Acta Part A, 60 (2004) 19–24.

[4] H.J. Tao, J. Zhang and X.L. Wang. Effect of diluents on the crystallization behavior of poly(4-methyl-1-pentene) and membrane morphology via thermally induced phase separation, J. Appl. Polym. Sci., 108 (2008) 1348–1355.
[5] H.J. Tao, J. Zhang, X.L. Wang and Z.Z. Xu, Phase separation and polymer crystallization in a poly(4-methyl-1-pentene)-dioctylsebacate-dimethylphthalate system via thermally induced phase separation, J. Polym. Sci. Part B: Polym. Phys., 45 (2007) 153–161.
[6] D.R. Lloyd, K.E. Kinzer and H.S. Tseng, Microporous membrane formation via thermally induced phase separation. I. solid-liquid phase separation, J. Membr. Sci., 52 (1990) 239–261.
[7] S.S. Kim and D.R. Lloyd, Microporous membrane formation via thermally induced phase separation. III. Effect of thermodynamic interaction on the structure of isotactic polypropylene membrane, J. Membr. Sci., 64 (1991) 13–29.
[8] G.B.A. Lim, S.S. Kim, Q. Ye, Y.F. Wang and D.R. Lloyd, Microporous membrane formation via thermally-induced phase separation. IV. Effect of isotactic polypropylene crystallization kinetics on membrane structure, J. Membr. Sci., 64 (1991) 31–40.
[9] S.S Kim, G.B.A. Lim, A.A. Alwattari, Y.F. Wang and D.R. Lloyd, Microporous membrane formation via thermally induced phase separation. V. Effect of diluent mobility and crystallization on the structure of isotactic polypropylene membranes, J. Membr. Sci., 64 (1991) 41–53.
[10] H. Matsuyama, H. Okafuji, T. Maki and N. Kubota, Preparation of polyethylene hollow fiber membrane via thermally induced phase separation, J. Membr. Sci., 223 (2003) 119–126.
[11] H. Matsuyama, T. Iwatani, Y. Kitamura, M. Tearamoto and N. Sugoh, Formation of porous poly(ethylene-co-vinyl alcohol) membrane via thermally induced phase separation, J. Appl. Polym. Sci., 79 (2003) 2449–2455.
[12] H. Matsuyama, K. Kobayashi, T. Maki, M. Tearamoto and H. Tsuruta, Effect of the ethylene content of poly(ethylene-co-vinyl alcohol) on the formation of microporous membranes via thermally induced phase separation, J. Appl. Polym. Sci., 82 (2001) 2583–2589.
[13] X.F. Li and X.L. Lu, Morphology of polyvinylidene fluoride and its blend in thermally induced phase separation process, J. Appl. Polym. Sci., 101 (2006) 2944–2952.
[14] J. Zhang, J.H. Fu, X.L. Wang, B.J. Wang, Z.Z. Xu, and J.Z. Wen, Effect of diluents on hydrophilic ethylene-acrylic acid copolymer membrane structure via thermally induced phase separation, Desalination, 192 (2006) 151–159.
[15] J. Zhang, X.L. Wang, F. Luo, H.L. Li and Z.Z. Xu, Formation of low density polyethylene microporous membrane via thermally induced phase separation (I) LDPE-18D/DPE system, Polym. Mater. Sci. Eng. (China), 20 (2004) 174–178.
[16] F. Luo, J. Zhang, X.L. Wang, J.F. Chen and Z.Z. Xu, Formation of hydrophilic ethylene-acrylic acid copolymer microporous membrane via thermally induced phase separation, Acta Polym. Sin., (2002) 566–571.
[17] Y.M. Dong, Polymer Analysis Handbook, China Petro Chemical Press, Beijing, 2004.
[18] B.Z. Luo, J. Zhang, X.L. Wang, Y. Zhou and J.Z. Wen, Effects of nucleating agents and extractants on the structure of polypropylene microporous membranes via thermally induced phase separation, Desalination, 192 (2006) 142–150.
[19] C.V. Raymond, and B. Seymour, Handbook of Polyolefins Synthesis and Properties, Marcel Dekker Inc., New York, 1993.
[20] G. Zhou, Polymer X-ray Diffraction, University of Science and Technology of China Press, Hefei, 1989.
[21] R.G. Jin and Y.Q. Hua, Polymer Physicis, Second Edition, Chemical Industry Press, Beijing, 2000.
[22] G. Charlet and G Delmas, Effect of solvent on the polymorphism of poly(4-methylpentene-1): 1. Solution-grown single crystals, Polymer, 25 (1984) 1613-1618.
[23] G. Charlet and G. Delmas, Effect of solvent on the polymorphism of poly(4-methylpentene-1): 2. Crystallization in semi-dilute solutions, Polymer, 25 (1984) 1619–1625.
[24] Y.S. Yadav and P.C. Jain, Melting behavior of isotactic polypropylene isothermally crystallized from the melt, Polymer, 27 (1986) 721–727.
[25] T. Pakula, Molecular model of partial crystallization of branched polyethylene, Polymer, 23 (1982) 1300–1304.
[26] J.L. Zryd and W.R. Burghardt, Phase separation, crystallization, and structure formation in immisicible polymer solutions, J. Appl. Polym. Sci., 57 (1995) 1525–1537.
[27] C.A. Avila-Orta, F.J. Medellín-Rodríguez, Z.G. Wang, D. Navarro-Rodríguez, B.S. Hsiao and F. Yeh, On the nature of multiple melting in poly(ethylene terephthalate)(PET) and its copolymers with cyclohexylene dimethylene terephthalate (PET/CT), Polymer, 44 (2003) 1527–1535.
[28] F.J. Medellin-Rodriguez, P.J. Phillips, J.S. Lin and R. Campos, The triple melting behavior of poly(ethylene terephthalate) molecular weight effects, J. Polym. Sci. Part B: Polym. Phys., 35 (1997) 1757–1774.
[29] S. Rastogi, G.W.H. Ho1hne, and A. Keller, Unusual pressure-induced phase behavior in crystalline poly(4-methylpentene-1): calorimetric and spectroscopic results and further implications, Macromolecules, 32 (1999) 8897–8909.